Atmospheric Environment xxx (2012) 1–10

Contents lists available at SciVerse ScienceDirect

Atmospheric Environment

journal homepage: www.elsevier.com/locate/atmosenv

Size resolved measurements of springtime aerosol particles over the northern South China Sea

Samuel A. Atwood [a], Jeffrey S. Reid [b,*], Sonia M. Kreidenweis [a], Steven S. Cliff [d], Yongjing Zhao [d], Neng-Huei Lin [c], Si-Chee Tsay [e], Yu-Chi Chu [f], Douglas L. Westphal [b]

[a] Department of Atmospheric Science, Colorado State University, 200 West Lake Street, Ft. Collins, CO 80523-1371, USA
[b] Aerosol and Radiation Section, Marine Meteorology Division, Naval Research Laboratory, Grace Hopper Ave., Stop 2, Monterey, CA 93943-5502, USA
[c] Department of Atmospheric Sciences, National Central University, Chung-Li, Taiwan
[d] Air Quality Research Center, University of California Davis, Davis, CA 95616, USA
[e] Goddard Space Flight Center, NASA, Greenbelt, MD, USA
[f] Taiwan Environmental Protection Administration, Taipei, Taiwan

HIGHLIGHTS

- The marine boundary layer aerosol was a mixture of pollution, dust and sea salt.
- Strong vertical wind shear decoupled transport across the boundary layer inversion.
- Aerosol optical thickness was largely uncorrelated with surface mass concentrations.

ARTICLE INFO

Article history:
Received 5 April 2012
Received in revised form
7 November 2012
Accepted 12 November 2012

Keywords:
Asian aerosol
Aerosol vertical distributions
Marine aerosol
Dust aerosol
Biomass burning aerosol

ABSTRACT

Large sources of aerosol particles and their precursors are ubiquitous in East Asia. Such sources are known to impact the South China Sea (henceforth SCS), a sometimes heavily polluted region that has been suggested as particularly vulnerable to climate change. To help elucidate springtime aerosol transport into the SCS, an intensive study was performed on the remote Dongsha (aka Pratas) Islands Atoll in spring 2010. As part of this deployment, a Davis Rotating-drum Uniform size-cut Monitor (DRUM) cascade impactor was deployed to collect size-resolved aerosol samples at the surface that were analyzed by X-ray fluorescence for concentrations of selected elements. HYSPLIT backtrajectories indicated that the transport of aerosol observed at the surface at Dongsha was occurring primarily from regions generally to the north and east. This observation was consistent with the apparent persistence of pollution and dust aerosol, along with sea salt, in the ground-based dataset. In contrast to the sea-level observations, modeled aerosol transport suggested that the westerly flow aloft (~700 hPa) transported smoke-laden air toward the site from regions from the south and west. Measured aerosol optical depth at the site was highest during time periods of modeled heavy smoke loadings aloft. These periods did not coincide with elevated aerosol concentrations at the surface, although the model suggested sporadic mixing of this free-tropospheric aerosol to the surface over the SCS. A biomass burning signature was not clearly identified in the surface aerosol composition data, consistent with this aerosol type remaining primarily aloft and not mixing strongly to the surface during the study. Significant vertical wind shear in the region also supports the idea that different source regions lead to varying aerosol impacts in different vertical layers, and suggests the potential for considerable vertical inhomogeneity in the SCS aerosol environment.

Published by Elsevier Ltd.

1. Introduction

The region surrounding the South China Sea (also known as the East Sea, henceforth SCS) is routinely impacted by aerosol outbreaks from the surrounding Asian regions (Lin et al., 2007a, 2009; Verma et al., 2009; Reid et al., 2009; Cohen et al., 2010a,b;

* Corresponding author. Tel.: +1 831 656 4725.
E-mail addresses: satwood@atmos.colostate.edu (S.A. Atwood), reidj@nrlmry.navy.mil, jeffrey.reid@nrlmry.navy.mil (J.S. Reid), sonia@atmos.colostate.edu (S.M. Kreidenweis), sscliff@ucdavis.edu (S.S. Cliff), yjzhao@ucdavis.edu (Y. Zhao), nhlin@cc.ncu.edu.tw (N.-H. Lin), si-chee.tsay@nasa.gov (S.-C. Tsay), ycchu@epa.gov.tw (Y.-C. Chu), douglas.westphal@nrlmry.navy.mil (D.L. Westphal).

1352-2310/$ – see front matter Published by Elsevier Ltd.
http://dx.doi.org/10.1016/j.atmosenv.2012.11.024

Wang et al., 2011). These papers showed that in the springtime in particular, the SCS is impacted from dust and pollution from China as well as biomass burning from Southeast Asia. These aerosol types may interact in a complex manner with the background marine aerosol environment. In addition to the obvious impacts on visibility and atmospheric radiative transfer, modeling studies of aerosol–cloud–precipitation interactions suggest that cloud systems such as those found in the SCS region may be susceptible to the introduction of smoke, dust and pollution particles (Sorooshian et al., 2009, 2010; Jiang et al., 2010; Yuan et al., 2011). At the same time, the Southeast Asian subcontinent may be among the most susceptible regions in the world to climate change (Yusef and Francisco, 2009). Understanding the nature, sources, and transport of particulate matter is thus critical to understanding the climate, visibility, and precipitation patterns in the region.

The potential for strong aerosol–cloud interactions in the SCS demonstrates the need to characterize particles and their sources in both the marine boundary layer (MBL) and in the free tropospheric air above it. Height dependent air masses with different particle loadings are transported into the area intermittently and are likely to contribute unequally to measured aerosol optical thickness (AOT) and composition. The remoteness of the SCS has resulted in relatively few measurements that are removed from the immediate influence of local sources, and thus few datasets are representative of the "regional" aerosol. Existing aerosol observations in the SCS are summarized by Chuang et al. (2012).

An opportunity arose in spring 2010 to sample aerosol particles entering the SCS. As part of the 7 SouthEast Asian Studies (7SEAS) campaign, the National Central University of Taiwan, supported by the Taiwan Environmental Protection Administration and the National Research Counsel, led an international field mission to study the transport of smoke and pollution from Indochina to Taiwan. As part of this project, a comprehensive supersite was deployed at Dongsha Island in the northern SCS (Wang et al., 2011; Lin et al., in this issue) from mid-March through mid-May, 2010. Prevailing low-level winds place Dongsha Island in a region which may be frequently impacted by Asian sources. In addition, there is minimal human activity on the island, so it is generally free of local pollution sources that would be more typical of mainland sites. The site thus provided a unique opportunity to study MBL aerosol composition and sources, and assess their representativeness of the larger SCS environment. The focus here is on using in-situ aerosol size and composition data, along with additional observations and model output, to identify transport patterns for aerosol affecting the SCS region. Using five weeks of data from a size-resolved aerosol cascade impactor, we look for elemental markers that may help identify specific sources. These data, combined with Navy Aerosol Analysis and Prediction System (NAAPS) aerosol reanalysis and NOAA HYSPLIT backward and forward trajectories, are used to analyze springtime aerosol sources and transport patterns in the northern SCS.

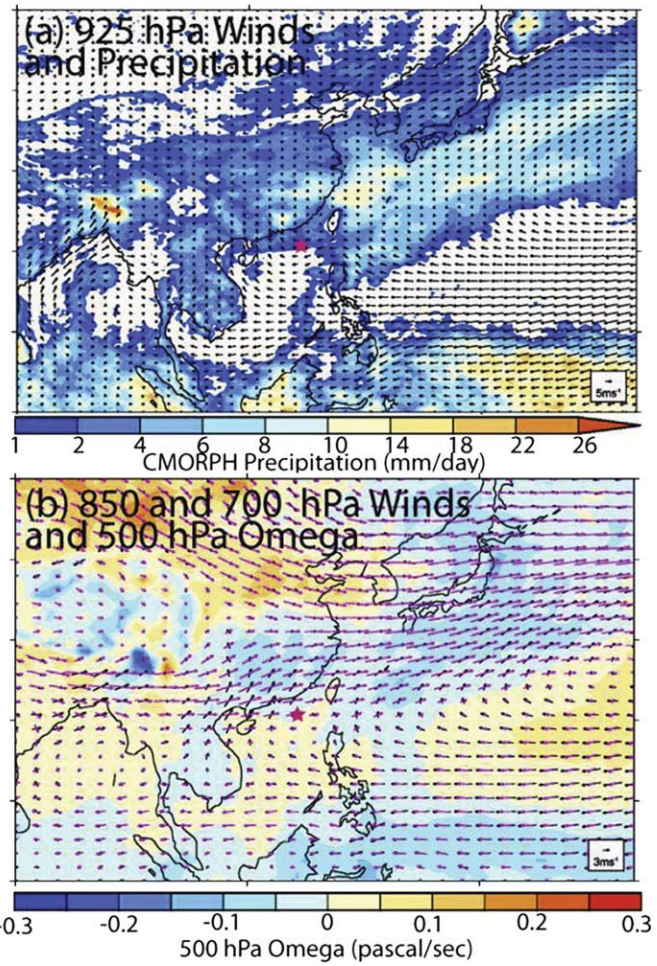

Fig. 1. (a) NOGAPS 925 hPa winds with CMORPH (CPC MORPHing technique (Joyce et al., 2004))Precipitation (mm day^{-1}) and (b) NOGAPS 850 (black) and 700 hPa (red) winds with 500 hPa Omega, for April 2010 during the Dongsha Experiment. Negative omega indicates regions of ascending motion; positive omega indicates regions of descending motion. (For interpretation of the references to color in this figure legend, the reader is referred to the web version of this article.)

2. Sampling site and methods

2.1. Site description

The Dongsha Islands (also known as the Pratas Islands; 20.7° N, 116.7° E) are a small group of low-lying islands forming an atoll located in the northern part the SCS (Fig. 1). Aerosol sources vary throughout the year, largely driven by changing winds associated with the East Asian Monsoon (Lin et al., 2007b). During the November through April winter monsoon season, prevailing winds from the northeast, associated with the passage of cold fronts, bring polluted air masses from regions in China, Japan, and the Korean Peninsula. Tan et al. (2012) and Wang et al. (2011) presented observations of Asian dust transport to the SCS under such meteorological conditions. For example, Ou-Yang et al. (2012) observed elevated ozone, associated with polluted air masses, at Dongsha in spring 2010, and demonstrated the existence of distinct layers in the atmosphere over the SCS in this season. During the spring, the low-level air masses in the SCS laden with Central Asian dust and East Asian pollution have been observed coincident with Southeast Asian biomass burning plumes aloft (Lin et al., 2007b; Wang et al., 2011; Reid et al., 2012; Ou-Yang et al., 2012). AOT in the SCS are generally highest during March and April, with averaged values ranging from 0.1 to 0.6 (Lin et al., 2007a). Onset of the summer monsoon in the SCS typically occurs in early to mid-May, bringing a reversal to low-level southwesterly winds.

Sampling was performed at the NASA COMMIT sampling trailer placed on the eastern side of the ~3 km × 1 km main island. A full description of the site and its instrumentation can be found in Wang et al. (2011); Lin et al. (in this issue); Bell et al. (2012); and Tsay et al. (in this issue). Chuang et al. (2012) conducted aerosol sampling at the site for two intensive periods, one of which (10–19 April 2010) overlapped with our study period. There are no indigenous inhabitants on the main island; however, a small population exists for research, fishing and military purposes, with no habitation on other islands in the atoll. The main island and the instrumentation were powered by a diesel generator, and an airstrip hosts flight operations

Please cite this article in press as: Atwood, S.A., et al., Size resolved measurements of springtime aerosol particles over the northern South China Sea, Atmospheric Environment (2012), http://dx.doi.org/10.1016/j.atmosenv.2012.11.024

once or twice per week. The locations for these sources are out of the prevailing wind directions for the sampling.

2.2. DRUM size-resolved aerosol samples

A free-standing eight-stage Davis Rotating-drum Uniform size-cut Monitor (DRUM) sampler was operated continuously in the COMMIT trailer from 31 March through 8 May 2010. The instrument used was a version of the DRUM sampler originally described by Cahill et al. (1985), modified to utilize slit orifices and configured to run at 16 L min^{-1} as described in Reid et al. (2008). An unheated PM_{10} sample inlet was used, followed by collection stages with 50% aerodynamic diameter cut sizes of 5 μm, 2.5 μm, 1.15 μm, 0.75 μm, 0.56 μm, 0.34 μm, 0.26 μm, and 0.07 μm, corresponding to Stages 1 through 8, respectively. Aerosol particles are collected on Mylar strips coated with Apiezon grease and wrapped around each rotating drum. The drums are then rotated at a consistent rate such that nominal timestamps can be assigned to specific locations along the strip during compositional analyses, yielding 3-h time resolution for the Dongsha deployment. Uniformity of the impacted sample was demonstrated by Bench et al. (2002).

DRUM samples were subjected to Synchrotron X-Ray Fluorescence (SXRF) analysis at the Advanced Light Source of Lawrence Berkeley National Laboratory to provide measurements of 27 elements having atomic weights between Mg and Mo, along with Pb (Van Curen et al., 2012; Perry et al., 2004). In Table 1 we indicate the 12 elements selected for further analysis in this study with estimated uncertainties. Reported uncertainty values were calculated based on the propagation of uncertainties from several inputs. A flow rate uncertainty and standard measurement value uncertainty of 5% each were used, along with analytical uncertainty from the SXRF data reduction algorithm, which varies for each element and for each size cut in the DRUM (Perry et al., 2004). Measurements below the minimum quantifiable limit were filtered out of the dataset.

The set of 12 elements was chosen to be consistent with the choices for a similar measurement campaign reported recently by Van Curen et al. (2012), and to include those elements that had the highest rates of valid data. As discussed at length in Van Curen et al. (2012), these elements are also associated with certain sources: Cl, Br, and Ca are marine-dominated; Ca, Al, Si, Fe, and Ti are terrestrial mineral elements; K is associated with mineral dust as well a frequently used as an indicator of biomass burning aerosol; Zn, Mo and Pb are associated with liquid fossil fuels; and S is primarily present as sulfate, which has a strong source from oxidation of anthropogenically-derived SO_2. We stress, however, that none of these elements is unique to any particular source.

Table 1
Elements detected by SXRF used in this analysis and the reported uncertainties, given as a percentage of the observed concentrations. All uncertainties are for Stage 2 species concentrations, except for S, for which the uncertainties on Stages 5 and 7, respectively, are shown. Mo and Pb were the only species that had any 3-h Stage 2 concentrations below detection limits. The last four columns show the ratios of each total measured elemental concentration that was in the $PM_{2.5}$ fraction (i.e., $PM_{2.5}$:PM_{10}), computed as a regression and slope, and also as the average ratio and its standard deviation (Stdev).

Element	Uncertainty, %	Ratio slope	r^2	Ratio average	Stdev
Cl	8%	0.39	0.58	0.32	0.13
Br	8%	0.67	0.85	0.71	0.04
Ca	7%	0.63	0.88	0.47	0.12
Al	13%	0.67	0.94	0.53	0.09
Si	9%	0.67	0.94	0.56	0.11
Fe	7%	0.72	0.96	0.55	0.13
Ti	7%	0.70	0.94	0.61	0.10
K	7%	0.74	0.96	0.60	0.11
Zn	7%	0.98	0.98	0.85	0.09
Mo	7%–50%	0.91	0.88	0.75	0.06
Pb	7%–96%	0.85	0.96	0.82	0.08
S	7%–12%, 7%	0.96	0.98	0.81	0.09

DRUM instruments, and cascade impactors in general, are known to be subject to several sampling artifacts, most notably a) the potential for particle bounce and shattering, thereby shifting collected mass from upper to lower stages and thus undersizing (Reid et al., 2003b); b) peak broadening on upper stages, leading to decreased time resolution for larger particles; c) matrix effects in the SXRF analyses, leading to an underestimate of lighter elements (Reid et al., 2003a); d) evolution of some reactive species on the collection strip, such as Cl; e) humidification of the sample during expansion in the jets, leading to particle growth by water uptake and impaction on a stage larger than the actual dry aerodynamic diameter (e.g., Fang et al., 1991). We applied the analysis techniques discussed in Reid et al. (2003a,b) and determined that sizing errors for all but the last of these possible artifacts were not significant in this study, and that the humidification artifact might shift the particles up by one stage, leading to sharp peaks in the size distribution.

2.3. Air mass backtrajectories

To establish air mass source regions expected for Dongsha during the study, backtrajectories were generated using the NOAA Hybrid Single Particle Lagrangian Integrated Trajectory (HYSPLIT) version 4.9 Model (Draxler and Hess, 1997, 1998; Draxler, 2004). The GDAS1, $1^\circ \times 1^\circ$ global meteorological dataset, generated for HYSPLIT from the Global Data Assimilation System model, was used to run 120 h backwards trajectories, starting every 3 h beginning with 0 UTC for all of the year 2010 at initial heights of 100 m, 1500 m, and 3000 m over the sampling site.

2.4. Additional model-derived and observational data

Output from the Navy Aerosol Analysis and Prediction System (NAAPS) is used in this work to qualitatively compare variations in observed aerosol concentrations to modeled variations. NAAPS is a global $1^\circ \times 1^\circ$ aerosol transport model maintained operationally by the U.S. Navy to support various operations and research (Reid et al., 2009). The emissions, transport, and sinks of sulfate, smoke, and dust are simulated. Speciated mass concentrations and aerosol optical thicknesses are predicted. AOT from MODIS observations are assimilated into the model (Zhang et al., 2008). We extracted NAAPS data for comparison with our observations from the grid point containing the Dongsha sampling site.

To assess regional precipitation, we utilize the NRL blended TRMM-microwave-geostationary product (Turk et al., 2008). Precipitation events in the region occurring during the study are shown with 24-h accumulated precipitation maps overlaid on the midday MTSAT-IR product.

For comparison purposes, we include in our presented time series PM_{10} and $PM_{2.5}$ tapered element oscillating microbalance (TEOM) data collected by the NASA/COMMIT (PM_{10}) trailer and Taiwan EPA mobile trailer ($PM_{2.5}$). An AERONET sun photometer was also located on the island (Holben et al., 1998). The daily average Level 2.0 Spectral Deconvolution Algorithm (SDA) Version 4.1 was used to generate total AOT estimates and the fine and coarse mode contributions to AOT at 500 nm (O'Neill et al., 2003).

3. Results

3.1. Dongsha modeling overview

To help understand the nature of transport in the SCS region, we begin with an analysis of winds and precipitation from the Navy

Please cite this article in press as: Atwood, S.A., et al., Size resolved measurements of springtime aerosol particles over the northern South China Sea, Atmospheric Environment (2012), http://dx.doi.org/10.1016/j.atmosenv.2012.11.024

Operational Global Atmospheric Prediction System (NOGAPS) operational model for April 2010 (Fig. 1) as well as the mean speciated NAAPS AOTs (Fig. 2). From these figures it is clear that during our study period, the SCS in general, and Dongsha Island in particular, was in a transitional region between the northern synoptic storm track and the dry Southeast Asian boreal winter monsoon. Boundary layer winds (as depicted by the 925 hPa winds) were generally light easterly/northeasterly. Above the boundary layer, winds backed to more westerly. This vertical wind shear implies geographically different air mass (and thus aerosol) sources as a function of height over the SCS. The geographical separation of major aerosol sources was very clear in the maps of modeled AOT in Fig. 2, where average AOTs across the SCS ranged from 0.1 to 0.8 during our study period. As is typical for this season (Lin et al., 2009; Reid et al., 2009) smoke from biomass burning in the dry Indochina region was transported with the west-southwesterly winds over northern Vietnam, Dongsha Island, and Taiwan, with eventual removal in the storm track. The shape of the Indochina smoke plume in Fig. 2c combined with the winds in Fig. 1, suggested that this plume was above the boundary layer. The lack of precipitation along the plume in the region (not shown) would be consistent with a relatively long lifetime for this smoke aerosol.

Surface winds suggest that air masses that generally originate in East Asia, in the region between the westerly storm track to the north and the monsoonal flows to the south, can advect into the SCS. The modeled dust AOTs in particular suggest that dust reached the SCS, apparently a common occurrence (Cohen et al., 2010a). Indeed, before this measurement set, a large dust outbreak was observed at the Dongsha site and reported by Wang et al. (2011). Somewhat surprisingly, NAAPS did not predict large sulfate concentrations, although it might be expected from the flow patterns in the region that pollution from East Asia should be transported as well as dust, although as reported by Lin et al. (2007) these air masses transport separately at different altitudes and can remain largely unmixed over long distances, but arriving within a few hours of each other at the receptor site. Receptor analyses in northern Vietnam suggest such combined dust and pollutant transport into the region is commonplace (Cohen et al., 2010a,b).

Fig. 3 presents a time-height cross-section of NOGAPS wind and humidity fields (Fig. 3a). NAAPS dust (Fig. 3b), smoke (Fig. 3c), and sulfate (Fig. 3d) concentrations at Dongsha Island, and total NAAPS AOT and AERONET AOT (Fig. 3e). HYSPLIT backtrajectories starting at Dongsha Island at 100, 1500, and 3000 m are presented in Fig. 4a, b and c, respectively. The cross-sections show that the transport of aerosol layers aloft were dominated by westerlies bringing air masses from Indochina, with a few isolated cases of frontal lifting indicative of a more northerly source. At the surface, a more episodic nature of aerosol transport was predicted over the northern SCS. The wind shear as depicted in Fig. 1 is more clear in Fig. 3a, with a delineation at approximately 800 hPa between surface east-northeasterlies and free-tropospheric westerlies.

Dust was modeled to be fairly ubiquitous in the atmosphere over Dongsha Island at heights up to 400 hPa, but generally at a modal height of 650 hPa. The strongest modeled dust events at the surface, however, occurred in association with a frontal passage on April 23. Smoke was modeled to be present over Dongsha only for the first half of the measurement period, with occasional intrusions into the boundary layer. As expected, smoke was generally modeled to be aloft, at a modal height of 700 hPa. Finally, anthropogenic sulfate was modeled to be present in low concentrations in the boundary layer nearly continuously over the study period, except for the period April 17–20. Interestingly, the strong surface dust event of April 23–26 also contained the highest modeled concentrations of sulfate aerosol.

In general, NAAPS AOT compared well to AERONET observations (Fig. 3e), with the exception of underestimates on March 10 and May 8, when Dongsha Island was just on the edge of an aerosol plume. This good comparison is expected, as operational NAAPS utilizes MODIS AOT data assimilation, and supports some confidence that NAAPS accurately captured the overarching sources of aerosol particles at Dongsha Island (e.g., Indochinese smoke, Asian dust and pollution). The AERONET fine/coarse spectral deconvolution showed that AOTs were dominated by the fine mode. Even during the dust event of April 24–26, transport of pollution along with the dust resulted in a fine-mode-dominated AOT. The largest AOT events as modeled by NAAPS (April 8, 17, and 27) did not have corresponding

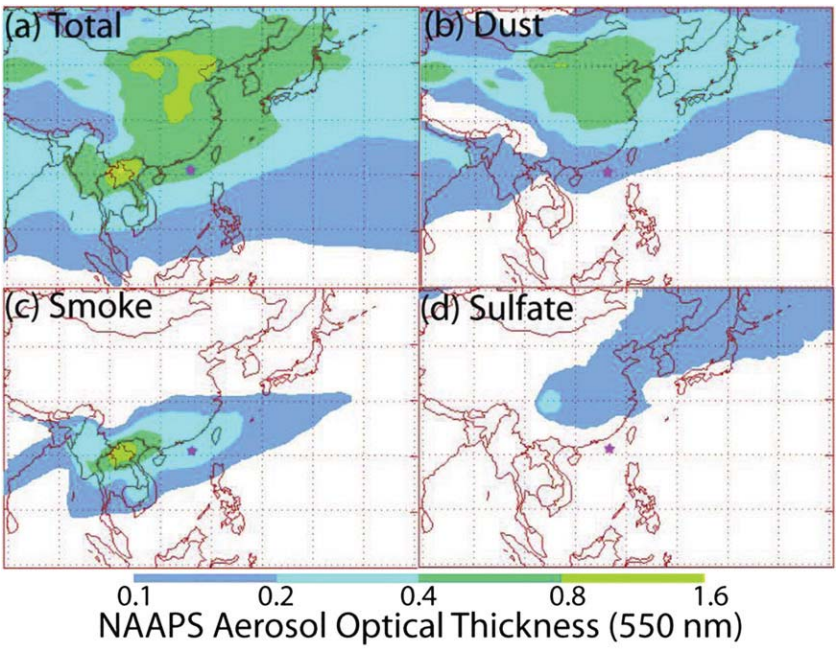

Fig. 2. Modeled NAAPS 550 nm AOT during the 31 March – 8 May, 2010 Dongsha Experiment for (a) total, (b) dust, (c) smoke, and (d) sulfate AOTs.

Please cite this article in press as: Atwood, S.A., et al., Size resolved measurements of springtime aerosol particles over the northern South China Sea, Atmospheric Environment (2012), http://dx.doi.org/10.1016/j.atmosenv.2012.11.024

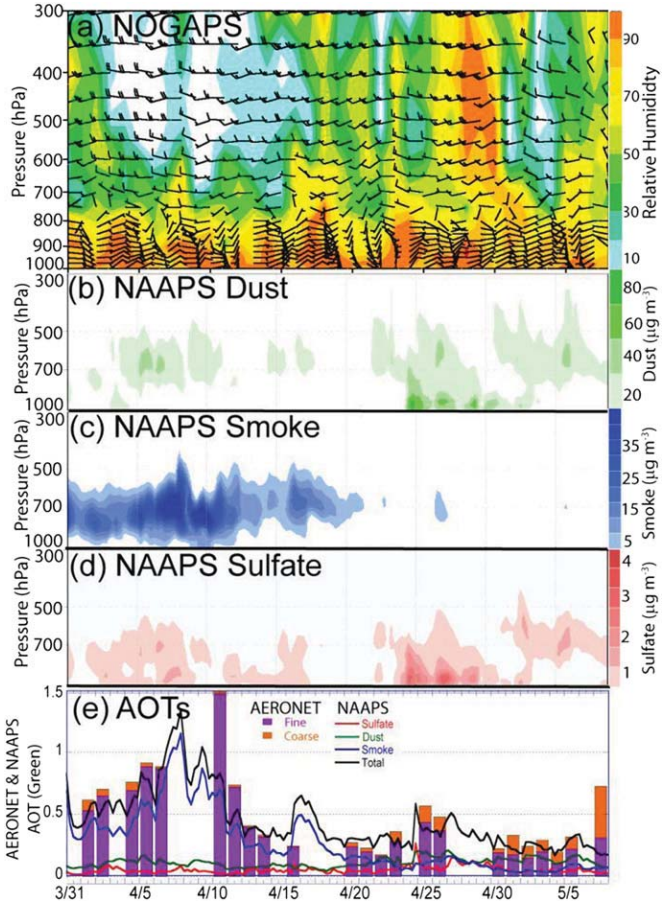

Fig. 3. (a) NOGAPS wind and RH profiles; modeled NAAPS (b) dust, (c) smoke, and (d) sulfate aerosol concentration profiles; (e) AERONET and NAAPS AOT contributions, for the grid box containing Dongsha Island.

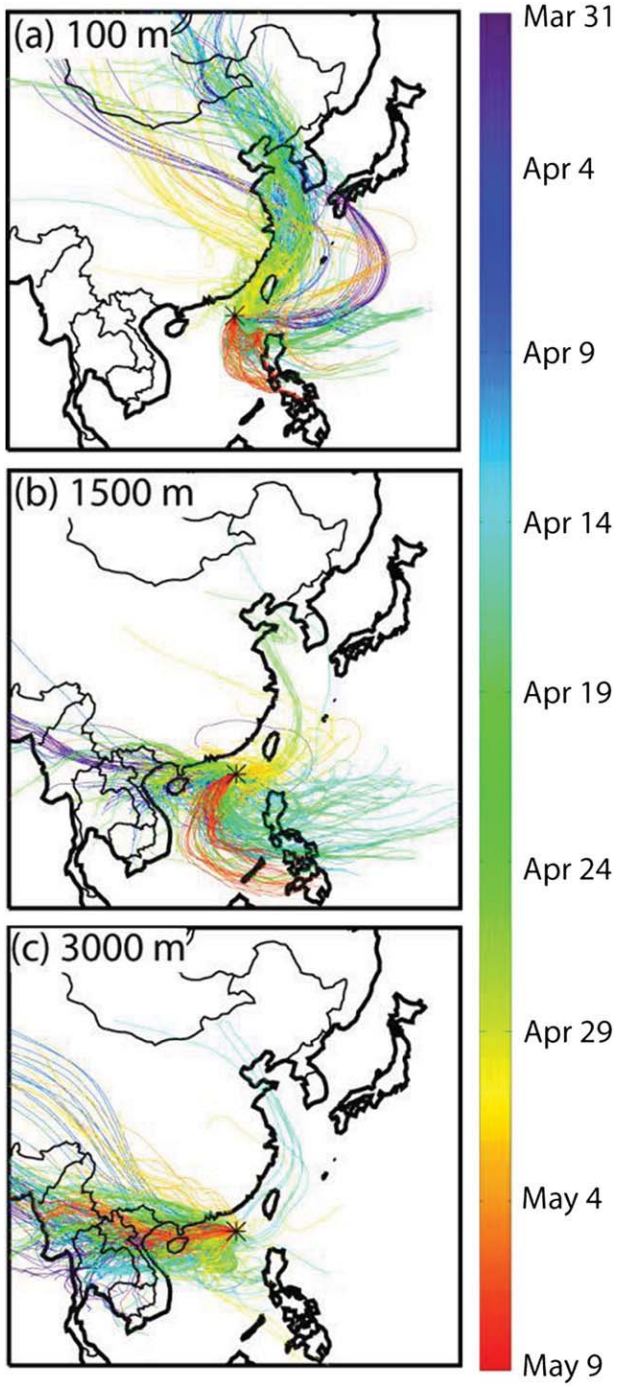

Fig. 4. HYSPLIT backtrajectories at (a) 100 m, (b) 1500 m, and (c) 3000 m receptor heights during the Dongsha Experiment. Color coding indicates date at which the backward calculation was initiated. (For interpretation of the references to color in this figure legend, the reader is referred to the web version of this article.)

AERONET data, suggesting that the transport of aerosol particles was associated with frontal activity and clouds, a fairly typical feature in frontal related transport (e.g., Zhang and Reid, 2009).

At finer scales and for sources influencing the boundary layer in remote regions, global models such as NAAPS, as well as bulk surface measurements such as PM_{10} and $PM_{2.5}$ aerosol mass concentrations, are not sufficient to support specific source attribution. For example, Fig. 5a presents NAAPS-simulated surface concentrations of dust, smoke and sulfate aerosols, and Fig. 5b presents TEOM-derived PM_{10} and $PM_{2.5}$ mass concentrations. NAAPS captured the transport of dust for the major event of April 24–30, but the overall signal-to-noise of small perturbations in most aerosol species for the rest of the period was so low that it was difficult to be definitive about sources impacting Dongsha Island and the SCS near the surface. Fig. 5b indicates that PM_{10} and $PM_{2.5}$ mass concentrations were highly correlated, with a nearly constant ratio of $PM_{2.5}/PM_{10}$ ~0.5, implying either transport covariance between coarse dust and/or sea salt and fine pollution/smoke particles, or the dominance of dust/sea salt in both size fractions. In either case, surface observations of $PM_{2.5}$ mass concentrations were largely useless as a metric for verification of the fine-mode components of modeled aerosol fields. We turn to size-resolved aerosol composition from the DRUM sampler to aid in the analysis.

3.2. Dongsha DRUM size distribution

Fig. 6 provides study-mean mass size distributions ($dM/d\ln d_{ae}$, $\mu g\ m^{-3}$) of selected elements. Provided are (a) the sum of all elemental mass concentrations; (b) sulfur (S), which as discussed above can be interpreted as primarily sulfate, a general indicator of anthropogenic emissions; (c) chlorine (Cl), which as discussed above can be interpreted as originating primarily from sea salt; (d) potassium (K), which is often used as a tracer for biomass burning but is also known to be associated with dust; and (e) iron (Fe), a key tracer for dust. Overall, the elemental size distributions for the DRUM data were tri-modal with strong peaks in Stage 2 (2.5–5 μm), Stage 5 (0.56–0.75 μm), and Stage 7 (0.26–0.34 μm). As

Please cite this article in press as: Atwood, S.A., et al., Size resolved measurements of springtime aerosol particles over the northern South China Sea, Atmospheric Environment (2012), http://dx.doi.org/10.1016/j.atmosenv.2012.11.024

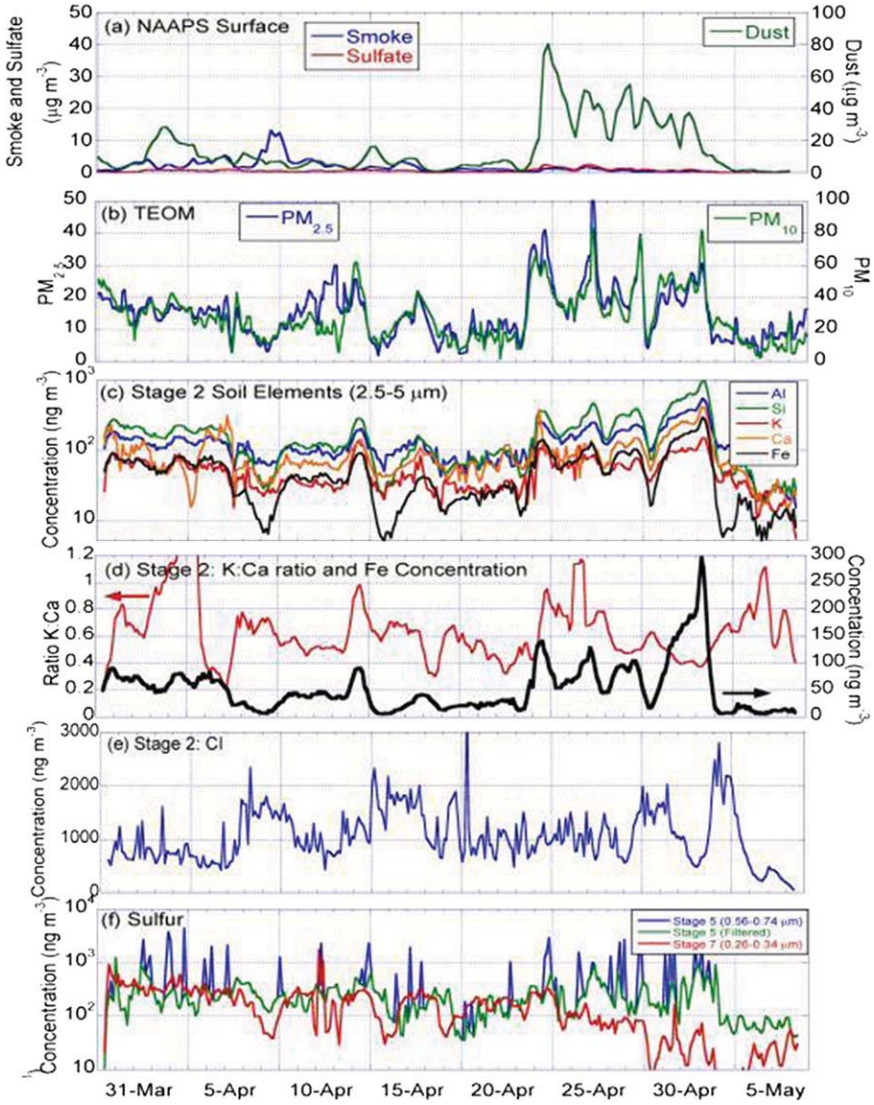

Fig. 5. (a) NAAPS surface smoke, sulfate, and dust concentrations for the grid box containing Dongsha Island; (b) TEOM PM_{10} and $PM_{2.5}$ mass concentrations; selected aerosol species from the DRUM sampling and SXRF analyses: (c) Stage 2 (2.5–5 μm) soil elemental concentrations, (d) Stage 2 K:Ca ratio and Fe concentration, (e) Stage 2 Cl, (f) Stage 5 (0.56–0.75 μm) and Stage 7 (0.26–0.34 μm) sulfur concentrations, and Stage 5 smoothed sulfur concentrations, with intermittent peaks filtered out.

expected, Fe and Cl, primarily from dust and sea salt, respectively, were found predominately in larger size fractions. Sulfur had concentration peaks in the accumulation (Stage 5) and ultrafine (Stage 7) fractions. Comparing the magnitude of the averaged summed mass distribution (Fig. 6a) with the distributions for S (Fig. 6b) and Cl (Fig. 6c), it is apparent that sulfate and sea salt likely constituted most of the $PM_{2.5}$ mass distribution, on average. This finding is consistent with the composition of $PM_{2.5}$ in Bell et al. (2012) for Dongsha during March and April 2010, namely, that non-sea-salt sulfate and sea salt dominated the fine aerosol composition. Nevertheless, most of the mass of sea salt was present in the coarse mode (Fig. 6c), and as shown by the mass distribution for iron in Fig. 6e, soil was also present in both the fine and the coarse modes, as also observed by Bell et al. (2012). The bulk of potassium was present in concentrations similar to those of iron at most size fractions, including larger $PM_{2.5}$. Potassium also had a small peak at ultrafine sizes (Stage 7) that could be indicative of biomass burning, but this peak did not constitute enough of a signal to differentiate it from the larger dust dominated contribution to K mass, so that identification of a biomass burning signal using this tracer was not possible.

The DRUM size data have important ramifications for interpretation of the $PM_{2.5}$ data. Based on the Fe and K size distributions provided in Fig. 6, we inferred that indeed a large fraction of the dust mass concentration was present in particles with aerodynamic diameters below the $PM_{2.5}$ cutoff. Table 1 provides the ratio of elemental $PM_{2.5}$:PM_{10} mass concentrations for all DRUM elements, computed two ways. First, to exhibit ratios for significant events, the ratio is provided as a regression slope and r^2. Also, straight averages and standard deviations are provided (i.e., all samples were equally weighted). As expected, species associated primarily with anthropogenic sources, such as sulfur, along with trace metals commonly attributable to combustion processes including diesel engines and smelting, such as zinc (Zn), molybdenum (Mo), and lead (Pb), were virtually nonexistent in the coarse mode. Generally, elements associated with dust, such as Al, Si and Fe, had $PM_{2.5}$:PM_{10} ratios on the order of 0.5–0.7. Cl, associated with sea salt, was mostly in the coarse mode (ratio 0.4); however, as discussed by Chuang et al. (2012), chlorine depletion was stronger in the fine mode than in the coarse mode, and thus its $PM_{2.5}$:PM_{10} ratio would be expected to be biased low. Hence, the strong correlations between $PM_{2.5}$ and PM_{10} concentrations in Fig. 5b could be clearly

Please cite this article in press as: Atwood, S.A., et al., Size resolved measurements of springtime aerosol particles over the northern South China Sea, Atmospheric Environment (2012), http://dx.doi.org/10.1016/j.atmosenv.2012.11.024

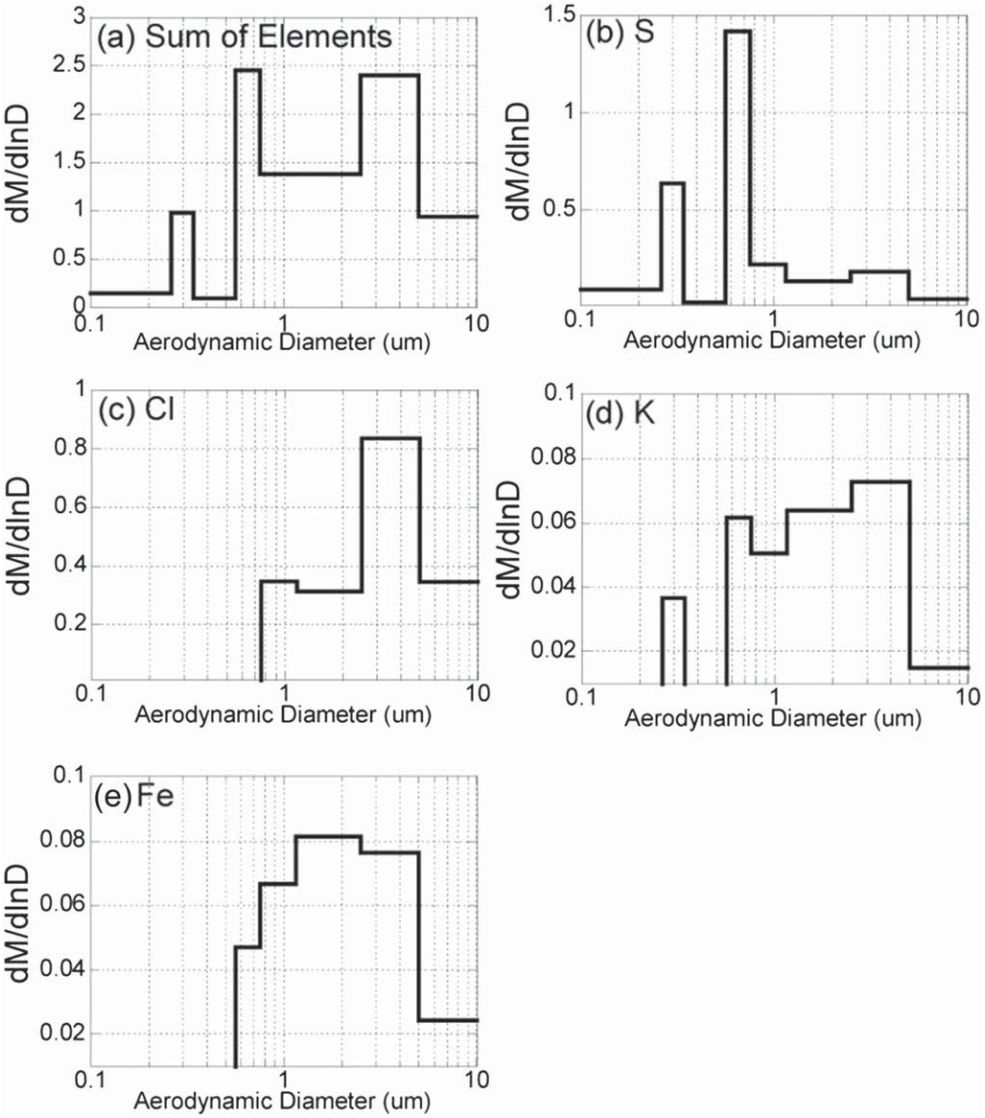

Fig. 6. DRUM mass size distributions (d*M*/d ln *D*) for (a) summed elements, (b) sulfur, (c) chlorine, (d) potassium, and (e) iron.

attributed to the presence of dust and sea salt in both modes. We can thus surmise that variations in $PM_{2.5}$ mass concentrations are dominated by variations in sea salt and dust aerosols, and unspeciated $PM_{2.5}$ mass concentrations alone are unlikely to be reliable direct indicators of anthropogenic pollution impacts at this site.

3.3. Time series of selected elements and elemental ratios

The previous size distribution analysis identified three aerosol size modes in the DRUM dataset: a coarse dust mode centered on Stage 2, a fine mass mode centered on Stage 5 and an ultrafine mass mode centered on Stage 7. Time series of selected elements and elemental ratios for these modes may thus be used to identify variations in aerosol types. Fig. 5c provides elemental concentrations on Stage 2 for Al, Si, K, Ca, and Fe; the ratio of K/Ca and concentration of Fe (linear scale) on Stage 2 are shown in Fig. 5d; and Stage 2 chlorine is shown in Fig. 5e as a general indicator of marine sea salt aerosol. Fine and ultrafine S timelines are shown in Fig. 5f.

First, temporal trends in Fe and other soil elements followed the TEOM data, again suggesting that dust, even in low total aerosol mass concentration conditions, strongly influenced $PM_{2.5}$ mass concentration variability. Chuang et al. (2012) found that on average, about 30% of the mass at Dongsha in both the fine and the coarse modes could not be speciated as either ionic or carbonaceous, which may also indicate the persistent presence of dust in both size fractions. The NAAPS-predicted extended dust event from 23 April–3 May is also clearly evident in the aerosol observations in Fig. 5: PM_{10} and $PM_{2.5}$ concentrations were elevated during this period (Fig. 5b), as were the soil-associated elements shown in Fig. 5c. In general, all of the soil-related elements tracked one another well throughout the study period, with correlations generally above 0.9. The one exception, however, was some deviations in the ratio of K to Ca (Fig. 5d), potentially an indicator of feldspars to carbonates (Reid et al., 2003a). During the largest dust peak, on May 3, as well as during the peak just prior to it (April 28–29), the mass concentration of Ca was roughly twice that of K, suggesting a more carbonate-enriched dust. Backtrajectories (100 m) during these periods show air mass source regions further inland over the western Gobi and Taklimakan deserts (blue backtrajectories, Fig. 7). However, during other events, the K:Ca ratio approached unity (e.g., April 4, 14, 24, 26) and backtrajectories

Please cite this article in press as: Atwood, S.A., et al., Size resolved measurements of springtime aerosol particles over the northern South China Sea, Atmospheric Environment (2012), http://dx.doi.org/10.1016/j.atmosenv.2012.11.024

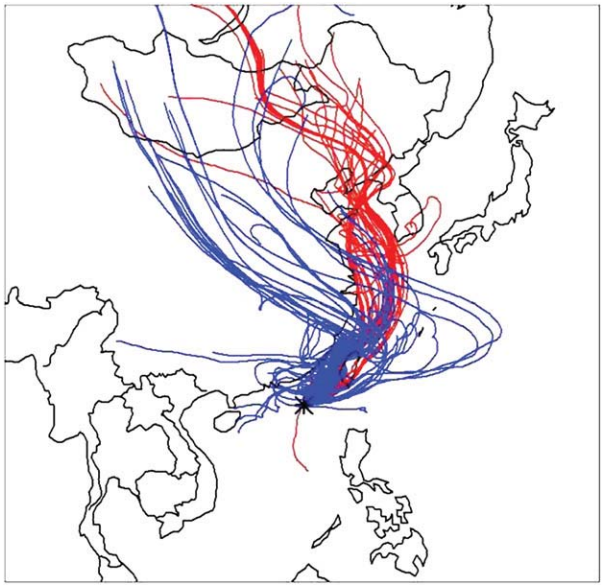

Fig. 7. Dongsha backtrajectories (100 m) during dust events with high K:Ca ratio (Apr 28, 29; May 1–3) shown in blue, and during dust events with low K:Ca ratio (Apr 4, 14, 24, 26) shown in red. (For interpretation of the references to color in this figure legend, the reader is referred to the web version of this article.)

indicated source regions from the eastern Gobi and coastal China (red backtrajectories, Fig. 7). That these variations in general synoptic transport patterns coincided with an indicator of dust type may indicate a difference in dust source regions during these events, as well as the possibility of different processing in the atmosphere along these different pathways.

Because Cl evolves in the atmosphere to HCl, it is not a conservative tracer for sea salt. However, the Cl time series should be a reasonable indicator of sea salt produced over the previous few days. Coarse mode chlorine (Fig. 5e) indicates that sea salt is nearly always present, with some variability in concentrations; higher-concentration episodes generally persist on the scale of ~2 days. The relatively low Cl mass concentrations and increased $PM_{2.5}$:PM_{10} ratio from April 10–13 was explained by Chuang et al. (2012) as having air masses originating from the Philippines, with sea salt aerosol largely depleted of chlorine. Overall, Chuang et al. (2012) found 60–80% chlorine depletion in the fine mode aerosol, and 51–96% depletion in the coarse mode. Thus DRUM-derived Cl would significantly underestimate the contribution of sea salt to the total aerosol mass concentrations.

Sulfur concentrations on Stage 5 were more variable, relative to those on Stage 7, and thus these stages were uncorrelated. The Stage 5 S spikes most often occurred only for a single time interval, although on a few occasions persisted for up to 3 intervals (9 h). We found that these concentrations spikes were strongly associated with Al (Al:S = 0.07; $r^2 = 0.97$) and K (K:S = 0.04; $r^2 = 0.90$), and less strongly with Ti (Ti:S = 0.0007; $r^2 = 0.57$), but had low correlations with other elements. Nominally, these elements can be indicative of fly ash, but the absence of correlation with other crustal elements, such as Si and Fe, that are often associated with fly ash (e.g., Hopke, 1991, 2003; Smichowski et al., 2005; Geng et al., 2010), is perplexing. A possibility is that these spikes may be a result of the intense shipping traffic in the region, rather than having coal burning as their primary source.

Particle concentration minima on April 9, 15 and May 4 are evident in the $PM_{2.5}$ and PM_{10} traces in Fig. 5b. During these periods, drops were measured in concentrations of soil elements, metals, and sulfur, along with TEOM mass, while chlorine mass concentrations (Fig. 5e) remained at typical levels and, together with associated marine sea salt elements, dominated particle mass fraction. Thus the air masses arriving at Dongsha clearly contained sea salt, but were reduced in mass concentrations of other aerosol types and thus could be classified as clean marine during these events. The Dongsha ozone data presented by Ou-Yang et al. (2012) also show minima at similar times. In Fig. 8, backtrajectories for these days are overlaid on the previous day's satellite based precipitation estimate from the NRL Blended product (Turk et al., 2008). Approximately 24 h into the backtrajectory, air parcels passed through observed precipitation regions which served to scrub them of pollution and dust that they may have been carrying. This analysis also lends some additional credence to the ability of HYSPLIT at the 100 m starting level to describe general synoptic transport patterns affecting Dongsha near the surface in the springtime.

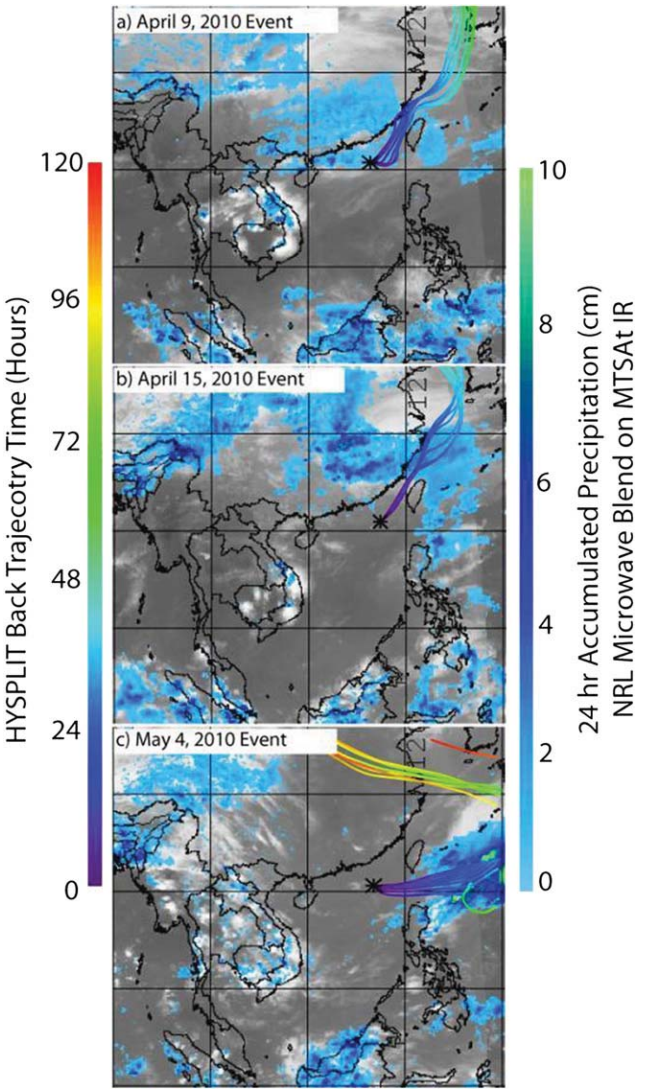

Fig. 8. Backtrajectories for aerosol particle concentration minima for (a) April 9, (b) April 15, and (c) May 5, 2010. Trajectories are placed on the previous day's 24 h accumulated NRL Blended precipitation product (Turk et al., 2008) and MTSAT-IR image.

4. Discussion and conclusions

We report findings from a study of springtime atmospheric aerosol characteristics at Dongsha Island in the South China Sea/East Sea, conducted between 31 March and 8 May 2010 as part of the larger 7SEAS campaign in Southeast Asia. Known aerosol types in East and Southeast Asia include dust, pollution, sea salt, and smoke from biomass burning (Lin et al., 2007a; Cohen et al., 2010a,b; Reid et al., 2012). Our measurements and model analysis sought to determine the varying, relative impacts of these aerosol sources both at the surface and in the vertical column above the site. The elements quantified in our surface-based samples by our analysis techniques were best suited to identification of aerosol from primary emissions, namely crustal elements associated with dust, metals typical of industrial pollution, and chlorine associated with sea salt. The elemental data showed that anthropogenic pollution and sea salt dominated surface aerosol during the early part of the study, while dust strongly impacted the site for about a week toward the end of April and into early May. We did not clearly identify smoke impacts in the surface-based chemical data. Potassium, a commonly applied tracer of biomass burning, was quantified in the SXRF analyses, but potassium is also associated with other types of sources such as dust that were frequently present in high concentration at the site. As a result, unequivocal attribution of surface aerosol to biomass burning sources was not possible.

Interestingly, considerable vertical wind shear in the SCS yielded significantly different backtrajectory source regions for air parcels arriving within, compared with those arriving above, the boundary layer over Dongsha, consistent with prior studies that also identified distinct atmospheric layers in springtime in this region (e.g., Lin et al., 2007b; Ou-Yang et al., 2012). Observations from the DRUM data along with a co-located TEOM sampling surface air, a co-located AERONET sun photometer measuring column extinction, and aerosol forecasts from the NAAPS model qualitatively confirmed the timing, magnitude, vertical distribution, and type of aerosol impacts at Dongsha. The combined information indicated that dust, sea salt, and pollution aerosols constituted higher fractions of the surface aerosol mass concentrations than throughout the rest of the column. In contrast, while smoke was likely a significant contributor to column aerosol loadings and AOT, it appeared to have only a minimal impact on aerosol concentrations at the surface. We note that Chuang et al. (2012) made measurements at Dongsha of aerosol organic and elemental carbon, as well as water-soluble, non-sea-salt K. They also saw no clear indication of the presence of biomass burning aerosol in their dataset, and also concluded that downward transport of smoke from the free troposphere to the surface at Dongsha was not significant during this study.

Based on these results, aerosol transport into the SCS in the springtime is understood to be generally dominated by low-level transport from regions throughout East Asia to the northwest, north, and northeast of Dongsha, while transport above the marine boundary layer originates in Southeast Asia to the island's west and southwest. Aerosol types that reached the surface at Dongsha during Spring 2010 were estimated to include dust from the Taklimakan and Gobi deserts of inland China and Mongolia; pollution from the major industrial and population centers of central and coastal China, Korea and Japan; and sea salt from marine areas surrounding the island, modified according to transport time and pathway. Based on basic measured and modeled column aerosol data, smoke from the highly-active biomass burning regions in Southeast Asia advected over Dongsha above the marine boundary layer following the general westerly flow patterns at those altitudes. The lack of a clear smoke-related potassium signal in the aerosol composition data, together with the NAAPS model predictions, indicated that smoke was largely sequestered above the marine boundary layer.

As backtrajectory analysis and seasonal climatology show generally consistent springtime transport within the SCS from year to year, the general conclusions from this study regarding aerosol source areas and types may represent a good general description of potential aerosol impacts at Dongsha for air masses arriving in the springtime. In agreement with previous studies in the region (e.g., Cohen et al., 2010a,b; Ou-Yang et al., in press; Tan et al., 2012) the results of this work indicate that the vertical inhomogeneity of the aerosol environment in the SCS is significant, and therefore the location and type of measurement (e.g., column vs. in situ in a specific layer of the atmosphere) should be considered during planning and analysis of measurements in the region.

Acknowledgments

This work was funded by the NRL Base Research Program and the Colorado State University Center for Geosciences/Atmospheric Research (CG/AR). The Dongsha field site, as part of the international 7SEAS activities, was funded by the Taiwanese Environmental Protection Administration and National Science Council, and by the NASA Radiation Sciences Program for the deployment of the COMMIT mobile laboratory. A portion of the analysis by Samuel Atwood was conducted as part of a Naval Research Enterprise Internship Program (NREIP). We are grateful for the support of the staff and students of the National Central University of Taiwan. We thank the NOAA Air Resources Laboratory for providing the HYSPLIT transport and dispersion model and the converted meteorological fields used in this publication. Finally, we would like to thank members of the Aerosol and Radiation Section for many useful conversations and help with data processing, including James Campbell, Cynthia Curtis, Walter Sessions, and Peng Xian-Lynch, as well as the ALS program including Kevin Perry.

References

Bell, S.W., et al., 2012. Constraining aerosol optical models using ground-based, collocated particle size and mass measurements in variable air mass regimes during the 7-SEAS/Dongsha Experiment. Atmospheric Environment. http://dx.doi.org/10.1016/j.atmosenv.2012.06.057.

Bench, G., Grant, P.G., Ueda, D., Cliff, S.S., Perry, K.D., Cahill, T.A., 2002. The use of STIM and PESA to measure profiles of aerosol mass and hydrogen content, respectively, across mylar rotating drums impactor samples. Aerosol Science and Technology 36, 642–651. http://dx.doi.org/10.1080/02786820252883874.

Cahill, T.A., Goodart, C., Nelson, J.W., Eldred, R.A., Nasstrom, J.S., Feeny, P.J., 1985. Design and evaluation of the DRUM impactor. In: Ariman, T., Nejat, T. (Eds.), Proceedings of the International Symposium on Particulate and Multiphase Processes, Washington, D. C., pp. 319–325.

Chuang, M.-T., et al., 2012. Aerosol chemical properties and related pollutants measured at Dongsha Island in the northern South China Sea during 7-SEAS/Dongsha Experiment. Atmospheric Environment. http://dx.doi.org/10.1016/j.atmosenv.2012.05.014.

Cohen, D.D., Crawford, J., Stelcer, E., Bac, V.T., 2010a. Characterization and source apportionment of fine particulate sources at Hanoi from 2001 to 2008. Atmospheric Environment 44, 320–328.

Cohen, D.D., Crawford, J., Stelcer, E., Bac, V.T., 2010b. Long range transport of fine particle windblown soils and coal fired power station emissions into Hanoi between 2001 to 2008. Atmospheric Environment 44, 3761–3769.

Draxler, R.R., Hess, G.D., 1997. Description of the HYSPLIT4 Modeling System. U.S. Dept. of Commerce, National Oceanic and Atmospheric Administration, Environmental Research Laboratories, Air Resources Laboratory, Silver Spring, Md.

Draxler, R.R., Hess, G.D., 1998. An overview of the HYSPLIT_4 modelling system for trajectories, dispersion and deposition. Australian Meteorological Magazine 47, 295–308.

Draxler, R.R., 2004. HYSPLIT4 Users's Guide. Available at: http://purl.access.gpo.gov/GPO/LPS47020 (accessed March 2012).

Fang, C.P., McMurry, P.H., Marple, V.A., Rubow, K.L., 1991. Effect of flow-induced relative-humidity changes on size cuts for sulfuric-acid droplets in the Microorifice Uniform Deposit Impactor (MOUDI). Aerosol Science and Technology 14, 266–277.

Geng, H., Kang, S., Jung, H.J., Choel, M., Kim, H., Ro, C.U., 2010. Characterization of individual submicrometer aerosol particles collected in Incheon, Korea, by quantitative transmission electron microscopy energy-dispersive X-ray spectrometry. Journal of Geophysical Research-Atmospheres 115, D15306. http://dx.doi.org/10.1029/2009JD013486.

Holben, B.N., Eck, T.F., Slutsker, I., Tanre, D., Buis, J.P., Setzer, A., Vermote, E., Reagan, J.A., Kaufman, Y.J., Nakajima, T., Lavenu, F., Jankowiak, I., Smirnov, A., 1998. AERONET – a federated instrument network and data archive for aerosol characterization. Remote Sensing of Environment 66, 1–16.

Hopke, P.K., 1991. An introduction to receptor modeling. Chemometrics and Intelligent Laboratory Systems 10, 21–43.

Hopke, P.K., 2003. Recent developments in receptor modeling. Journal of Chemometrics 17, 255–265.

Jiang, H.L., Feingold, G., Sorooshian, A., 2010. Effect of aerosol on the susceptibility and efficiency of precipitation in warm trade cumulus clouds. Journal of the Atmospheric Sciences 67, 3525–3540.

Joyce, R.J., Janowiak, J.E., Arkin, P.A., Xie, P.P., 2004. CMORPH: a method that produces global precipitation estimates from passive microwave and infrared data at high spatial and temporal resolution. Journal of Hydrometeorology 5, 487–503.

Lin, I.-I., Chen, J.P., Wong, G.T.F., Huang, C.-W., Lien, C.-C., 2007. Aerosol input to the South China Sea: results from the moderate resolution imaging spectroradiometer, the quick scatterometer, and the measurements of pollution in the troposphere sensor. Deep-Sea Research II 54, 1589–1601.

Lin, I.I., Chen, J.P., Wong, G.T.F., Huang, C.W., Lien, C.C., 2007a. Aerosol input to the South China Sea: results from the MODerate resolution Imaging Spectroradiometer, the quick scatterometer, and the measurements of pollution in the troposphere sensor. Deep-Sea Research Part Ii-Topical Studies in Oceanography 54, 1589–1601.

Lin, C.-Y., Wang, Z., Chen, W.-N., Chang, S.-Y., Chou, C.C.K., Sugimoto, N., Zhao, X., 2007b. Long-range transport of Asian dust and air pollutants to Taiwan: observed evidence and model simulation. Atmospheric Chemistry and Physics 7, 423–434.

Lin, C.Y., Hsu, H.M., Lee, Y.H., Kuo, C.H., Sheng, Y.F., Chu, D.A., 2009. A new transport mechanism of biomass burning from Indochina as identified by modeling studies. Atmospheric Chemistry and Physics 9, 7901–7911.

Lin, N.H., et al. An overview of regional experiments on biomass burning aerosols and related pollutants in Southeast Asia: 7SEAS/Dongsha experiment. Atmospheric Environment, in this issue.

O'Neill, N.T., Eck, T.F., Smirnov, A., Holben, B.N., Thulasiraman, S., 2003. Spectral discrimination of coarse and fine mode optical depth. Journal of Geophysical Research-Atmospheres 108, 15.

Ou-Yang, C.-F., et al., 2012. Influence of Asian continental outflow on the regional background ozone level in northern South China Sea. Atmospheric Environment. http://dx.doi.org/10.1016/j.atmosenv.2012.07.040.

Perry, K.D., Cliff, S.S., Jimenez-Cruz, M.P., 2004. Evidence for hygroscopic mineral dust particles from the intercontinental transport and chemical transformation experiment. Journal of Geophysical Research 109. http://dx.doi.org/10.1029/2004JD004979.

Reid, E.A., Reid, J.S., Meier, M.M., Dunlap, M.R., Cliff, S.S., Broumas, A., Perry, K., Maring, H., 2003a. Characterization of African dust transported to Puerto Rico by individual particle and size segregated bulk analysis. Journal of Geophysical Research-Atmospheres 108, D198591. http://dx.doi.org/10.1029/2002JD002935.

Reid, J.S., Jonsson, H.H., Maring, H.B., Smirnov, A., Savoie, D.L., Cliff, S.S., Reid, E.A., Livingston, J.M., Meier, M.M., Dubovik, O., Tsay, S.C., 2003b. Comparison of size and morphological measurements of coarse mode dust particles from Africa. Journal of Geophysical Research-Atmospheres 108, D198593. http://dx.doi.org/10.1029/2002JD002485.

Reid, J.S., Reid, E.A., Walker, A., Piketh, S., Cliff, S., Al Mandoos, A., Tsay, S.C., Eck, T.F., 2008. Dynamics of southwest Asian dust particle size characteristics with implications for global dust research. Journal of Geophysical Research-Atmospheres 113, D14212. http://dx.doi.org/10.1029/2007JD009752.

Reid, J.S., Hyer, E.J., Prins, E.M., Westphal, D.L., Zhang, J.L., Wang, J., Christopher, S.A., Curtis, C.A., Schmidt, C.C., Eleuterio, D.P., Richardson, K.A., Hoffman, J.P., 2009. Global monitoring and forecasting of biomass-burning smoke: description of and lessons from the Fire Locating and Modeling of Burning Emissions (FLAMBE) program. IEEE Journal of Selected Topics in Applied Earth Observations and Remote Sensing 2, 144–162.

Reid, J.S., Hyer, E.J., Johnson, R., et al., 2012. Observing and understanding the Southeast Asian aerosol system by remote sensing: an initial review and analysis for the Seven Southeast Asian Studies (7SEAS) program. Atmospheric Research. http://dx.doi.org/10.1016/j.atmosres.2012.06.005.

Smichowski, P., Polla, G., Gomez, D., 2005. Metal fractionation of atmospheric aerosols via sequential chemical extraction: a review. Analytical and Bioanalytical Chemistry 381, 302–316.

Sorooshian, A., Feingold, G., Lebsock, M.D., Jiang, H.L., Stephens, G.L., 2009. On the precipitation susceptibility of clouds to aerosol perturbations. Geophysical Research Letters 36, L13803. http://dx.doi.org/10.1029/2009GL038993.

Sorooshian, A., Feingold, G., Lebsock, M.D., Jiang, H.L., Stephens, G.L., 2010. Deconstructing the precipitation susceptibility construct: improving methodology for aerosol-cloud precipitation studies. Journal of Geophysical Research-Atmospheres 115, D17201. http://dx.doi.org/10.1029/2009JD013426.

Tan, S.-C., Shi, G.Y., Wang, H., 2012. Long-range transport of spring dust storms in inner Mongolia and impact on the China seas. Atmospheric Environment 46, 299–308.

Tsay, S.-C., Hsu, N.C., Lau, W.K.-M., et al. From BASE-ASIA towards 7-SEAS: a surface-satellite perspective of boreal spring biomass-burning aerosols and clouds in Southeast Asia. Atmospheric Environment, in this issue.

Turk, F.J., Arkin, P., Ebert, E.E., Sapiano, M.R.P., 2008. Evaluating high-resolution precipitation products. Bulletin of the American Meteorological Society 89, 1911–1916.

Van Curen, R.A., Cahill, T., Burkhart, J., Barnes, D., Zhao, Y., Perry, K., Cliff, S., McConnell, J., 2012. Aerosols and their sources at Summit Greenland – first results of continuous size- and time-resolved sampling. Atmospheric Environment 52, 82–97.

Verma, S., Worden, J., Payra, S., Jourdain, L., Shim, C., 2009. Characterizing the long-range transport of black carbon aerosols during Transport and Chemical Evolution over the Pacific (TRACE-P) experiment. Environmental Monitoring and Assessment 154, 85–92.

Wang, S.H., Tsay, S.C., Lin, N.H., Hsu, N.C., Bell, S.W., Li, C., Ji, Q., Jeong, M.J., Hansell, R.A., Welton, E.J., Holben, B.N., Sheu, G.R., Chu, Y.C., Chang, S.C., Liu, J.J., Chiang, W.L., 2011. First detailed observations of long-range transported dust over the northern South China Sea. Atmospheric Environment 45, 4804–4808.

Yuan, T.L., Remer, L.A., Pickering, K.E., Yu, H.B., 2011. Observational evidence of aerosol enhancement of lightning activity and convective invigoration. Geophysical Research Letters 38, L04701. http://dx.doi.org/10.1029/2010GL046052.

Yusef, A.A., Francisco, H., June 2009. Climate Change Vulnerability Mapping for Southeast Asia, Economy and Environment Program for Southeast Asia (EEPSEA) Report, 32 pp. Available at: http://www.eepsea.org.

Zhang, J.L., Reid, J.S., 2009. An analysis of clear sky and contextual biases using an operational over ocean MODIS aerosol product. Geophysical Research Letters 36, L15824. http://dx.doi.org/10.1029/2009GL038723.

Zhang, J.L., Reid, J.S., Westphal, D.L., Baker, N.L., Hyer, E.J., 2008. A system for operational aerosol optical depth data assimilation over global oceans. Journal of Geophysical Research-Atmospheres 113, D10208. http://dx.doi.org/10.1029/2007JD009065.

Please cite this article in press as: Atwood, S.A., et al., Size resolved measurements of springtime aerosol particles over the northern South China Sea, Atmospheric Environment (2012), http://dx.doi.org/10.1016/j.atmosenv.2012.11.024